

# Wavefront Analysis of High-Efficiency, Large-Scale, Thin Transmission Gratings

Chun Zhou<sup>1,4,\*</sup>, Takashi Seki<sup>2</sup>, Tsuyoshi Kitamura<sup>2</sup>, Yoshiyuki Kuramoto<sup>2</sup>, Takashi Sukegawa<sup>2</sup>, Nobuhisa Ishii<sup>3</sup>, Teruto Kanai<sup>3</sup>, Jiro Itatani<sup>3</sup>, Yohei Kobayashi<sup>3</sup>, and Shuntaro Watanabe<sup>1,4</sup>

<sup>1</sup>Research Institute for Science and Technology, Tokyo University of Science, Noda, Chiba 278-8510, Japan

<sup>2</sup>Corporate R&D Headquarters, CANON Inc., Utsunomiya 321-3292, Japan

<sup>3</sup>Institute for Solid State Physics, University of Tokyo, Kashiwa, Chiba 277-8581, Japan

<sup>4</sup>CREST, Japan Science and Technology Agency (JST), Chiyoda, Tokyo 102-0075, Japan

\*czhou@rs.noda.tus.ac.jp

**Abstract:** Large-scale transmission gratings with groove densities of 1250 and 1740 lines/mm have been developed with diffraction efficiencies above 95%. The minimized bending of the grating results in a negligible wavefront distortion of a pulse compressor.

**OCIS codes:** (050.0050) Diffraction and gratings; (320.7090) Ultrafast lasers.

## 1. Introduction

High-peak-power, ultrashort-pulse lasers with a high repetition rate are required in the generation of high-order harmonics and attosecond pulses [1]. Large-scale, high efficiency transmission gratings (TGs) are attractive for a compressor of terawatt (TW)-class Ti:sapphire lasers because of high damage threshold and long lifetime.

Here, we developed new TGs with a size of  $180 \times 60 \times 1 \text{ mm}^3$  and groove densities of 1740 and 1250 lines/mm by using optical lithography [2]. Both gratings showed diffraction efficiencies above 95% and a compressor throughput up to 80%. Thin grating reduces the threshold of white-light continuum generation due to self-phase modulation, but is easily bended by anti-reflection (AR) coating. We characterized the bending of a grating due to the AR coating by measuring the wavefronts of the reflected beams from the substrate surface. By improving the evaporation process, the bending due to AR coating was minimized to  $2.9 \lambda$  at 633 nm. The wavefront distortion of a pulse compressor is analyzed numerically.

## 2. Design and diffraction efficiencies of transmission gratings

We used a conventional projection system for semiconductor lithography to fabricate the TGs. The original pattern was exposed to a resist on a 1-mm-thick fused quartz substrate with a diameter of 200 mm by a  $4\times$  reduction lens system, and the size of one grating unit was  $10 \text{ mm} \times 10 \text{ mm}$ . The  $180 \text{ mm} \times 60 \text{ mm}$  grating is made by continuously connecting the  $18 \times 6$  matrices of one unit to form a single grating with an accuracy of 5 nm. The grooves are notched by etching the pattern on a fused quartz substrate. The back side of the grooves is AR coated.

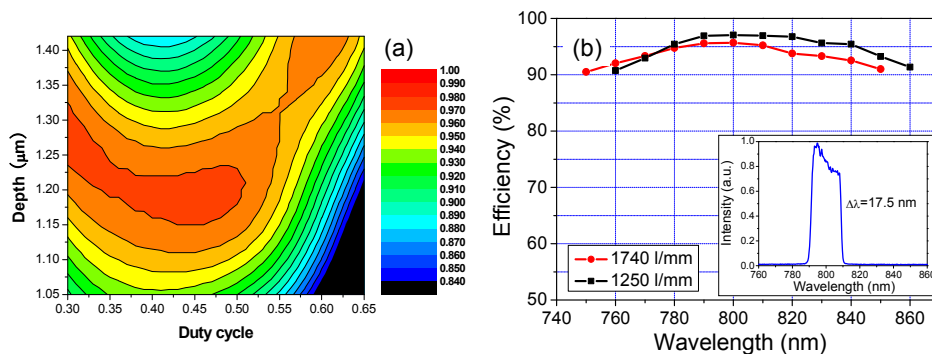


Fig. 1. (a) Calculated contour map of the efficiencies at 800 nm for a 1740-lines/mm grating. (b) Dependences of the diffraction efficiencies on the wavelength for the TE polarization in 1740- (red) and 1250- (black) lines/mm gratings. The inset shows a typical spectrum of the probe.

Figure 1(a) shows the calculated contour map of the efficiency at an incident angle of  $44^\circ$  with a 1740-lines/mm grating. The wavelength dependences of the diffraction efficiencies are shown in Fig. 1(b) for 1740 and 1250 lines/mm at incident angles of  $44^\circ$  and  $30^\circ$ , respectively. The maximum efficiency was over 95% at 800 nm. In the case of the 1250-lines/mm grating, efficiency reaches up to 97% at 800 nm and a compressor throughput is above 80% for 20 fs pulses.

### 3. Spatial distortion of transmission grating

The grating is held at the four corners by pressing to polished flat planes ( $1 \times 1 \text{ mm}^2$ ) by elastic plates. To determine the deformation of the TGs, we measured the wavefront distortion of the beam reflected from a TG by a Zygo interferometer equipped with a He-Ne laser (633 nm). The two-dimensional (2-D) wavefront distortion  $W(x, y)$  is related to the deformation of the grating  $H(x, y)$  by  $W(x, y) = 2H(x, y)$ , where  $x$  and  $y$  are the axes across and along the groove direction, respectively. For simplicity, we define  $W(x)$  as the average of  $W(x, y)$  from  $y = 27.5$  to  $32.5$  mm and  $H(x)$  represents the one-dimensional (1-D) distortion.

We observed a clear parabolic bending of the grating with AR coating by the ion-assisted deposition method. The bending direction was from the groove to AR surface (positive). The peak to valley (PV) values of the bending over the total area are distributed from  $44$  to  $52 \lambda$  at  $633 \text{ nm}$  among 5 samples with 1250- and 1740-lines/mm groove densities. The bending was reduced by one order of magnitude by adding a negative bending with a  $\text{SiO}_2$  under coat and by AR coating with e-beam deposition. Figure 2(a) and (b) show a 2-D wavefront map of  $W(x, y)$  and a profile in the central region  $W(x)$ , respectively. The bending is considerably reduced to  $\text{PV} = 2.9 \lambda$  in  $H(x)$  [ $\text{PV} = 5.8 \lambda$  in  $W(x)$ ].

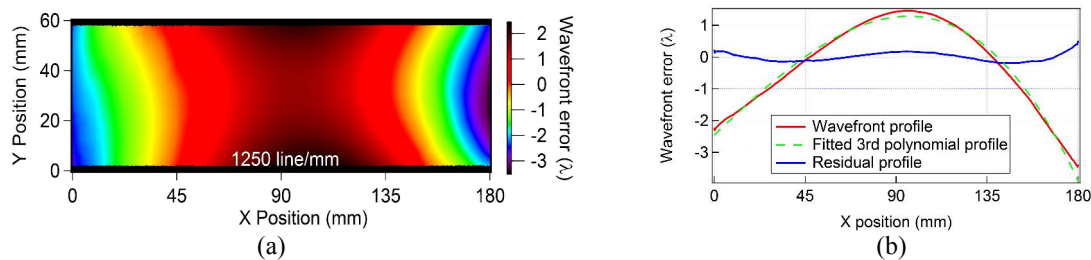


Fig. 2. (a) Reflected wavefront map of a grating with a groove density of 1250 lines/mm at 633 nm. (b) Wavefront profile (red solid line) averaged from  $y = 27.5$ – $32.5$  mm and fitted to a 3<sup>rd</sup>-order polynomial curve (green dash line).

### 4. Wavefront analysis and summary

By a simply analysis,  $W(x) = 2(\cos\beta_0 - \cos\alpha_0)H(x)$  for a double-passed TG, while  $W(x) = 2(\cos\beta_0 + \cos\alpha_0)H(x)$  for a reflective grating (RG), where  $\beta_0$  and  $\alpha_0$  are the diffracted and incident angles, respectively. This relation shows that the spatial bending can be canceled out through the TG in the Littrow condition of a monochromatic beam, while the wavefront distortion is approximately two times the spatial bending in the case of a RG. The wavefronts are almost flat in TG but largely parabolic in RG respectively as in Fig. 3(a) near the Littrow condition. Although femtosecond pulses contain a broad spectrum, this fact explains why a pulse compressor with TGs is considerably less sensitive to the bending than that of RGs.

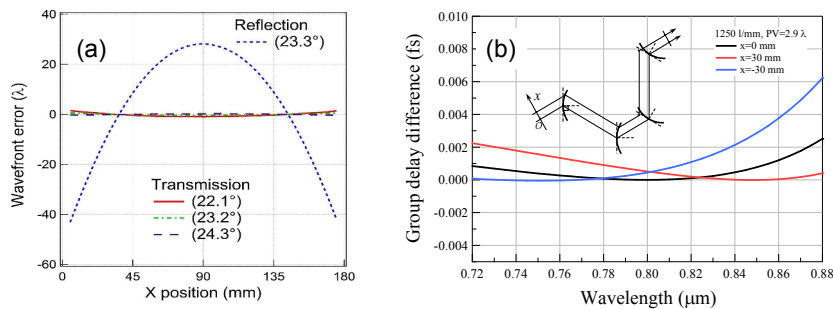


Fig. 3. (a) Wavefront errors in  $\lambda$  at 633 nm versus grating position along the dispersive direction for TG and RG, respectively.  $\text{PV} = 44 \lambda$  in  $H(x)$ . (b) Group delay differences relative to the flat grating pair for three different beam positions in the compressor with four TGs bended in the same direction along the beam.

Ray tracing calculation based on the measured bending shows that the group delay between 750 and 850 nm can be compensated within the spatial variation of  $<0.3 \text{ fs}$  in a folded compressor and  $<0.003 \text{ fs}$  in a four-grating compressor using 1250-lines/mm gratings for a 60-mm-diameter beam with a bandwidth of 100 nm as shown in Fig. 3(b). We measured the spatial pulse front distortion in a TW-class Ti:sapphire laser in which the beam size in the dispersive direction was 85 mm on a grating. However, we did not observe an apparent distortion across a 20-mm-diameter beam within a detection limit ( $<1.5 \text{ fs}$ ). This is consistent with the above ray tracing analysis.

[1] F. Krausz, and M. Ivanov, "Attosecond physics," Rev. Mod. Phys. **81**, 163-234 (2009).

[2] C. Zhou, T. Seki, T. Sukegawa, T. Kanai, J. Itatani, Y. Kobayashi, and S. Watanabe, "Large-scale, high-efficiency transmission grating for terawatt-class Ti:sapphire lasers at 1 kHz," Appl. Phys. Express **4**, 072701 (2011).